

Recent advances in the research of inorganic nanotubes and fullerene-like nanoparticles

Reshef Tenne

Department of Materials and Interfaces, Weizmann Institute, Rehovot 76100, Israel

E-mail: reshef.tenne@weizmann.ac.il

Received February 22, 2013; accepted March 25, 2013

This minireview outlines the main scientific directions in the research of inorganic nanotubes (INT) and fullerene-like (IF) nanoparticles from layered compounds, in recent years. In particular, this review describes to some detail the progress in the synthesis of new nanotubes, including those from misfit compounds; core-shell and the successful efforts to scale-up the synthesis of WS₂ multiwall nanotubes. The high-temperature catalytic growth of nanotubes, via solar ablation is discussed as well. Furthermore, the doping of the IF-MoS₂ nanoparticles and its influence on the physico-chemical properties of the nanoparticles, including their interesting tribological properties are briefly discussed. Finally, the numerous applications of these nanoparticles as superior solid lubricants and for reinforcing variety of polymers are discussed in brief.

Keywords inorganic nanotubes, fullerene-like (IF), nanomaterials, solid state chemistry

PACS numbers 61.66.Fn, 62.20.Qp, 68.37.Lp, 73.63.Fg, 81.40.Pq

Contents

1	Introduction	370
2	Large-scale synthesis of WS ₂ nanotubes	371
3	Doping of IF/INT-MoS ₂ (WS ₂)	372
4	Catalytic growth of metal-chalcogenide nanotubes	373
5	Growth of nanotubes from misfit compounds: (SnS) _n /(SnS ₂) _m nanotubes	374
6	Core-shell nanotubes	375
7	Applications	376
	Acknowledgements	376
	References and notes	376

1 Introduction

The discovery of inorganic nanotubes and fullerene-like nanoparticles [1, 2] nicknamed IF and INT, respectively, more than two decades ago, opened new research direction in solid state chemistry and in nanomaterials. Furthermore, the research into IF and INT offered numerous applications which develop steadily with new products gradually penetrating the market place. In

essence, it was hypothesized that nanophases of layered (two dimensional, 2D) compounds are unstable in their macroscopic form and they spontaneously fold to form closed-cage structures with large hollow core. Inorganic compounds with layered structure are abundant among binary metal chalcogenides; sub-stoichiometric oxides; halides and pnictides and also in variety or ternary compounds. In the bulk form they appear as planar crystallites (platelets). Each platelet is made of molecular sheets held together by weak van der Waals forces. Typical examples for such compounds are MoS₂, CdCl₂, H₂Ti₃O₇, NiPS₃ and more. It was suggested [1, 2] that, in analogy to the case of graphite, nanostructures of such compounds will form hollow closed structures akin to carbon fullerenes and nanotubes. Figure 1 shows the transmission electron microscope (TEM) image of (a) multiwall IF-MoS₂ nanoparticles, and WS₂ nanotube (INT-WS₂) of type I (b) and type II (c).

IF and INT from numerous layered compounds have been reported over the years. Various synthetic strategies have been developed or adapted for the synthesis of such nanostructures. The purpose of the present perspective is to shed light on recent developments in this field.

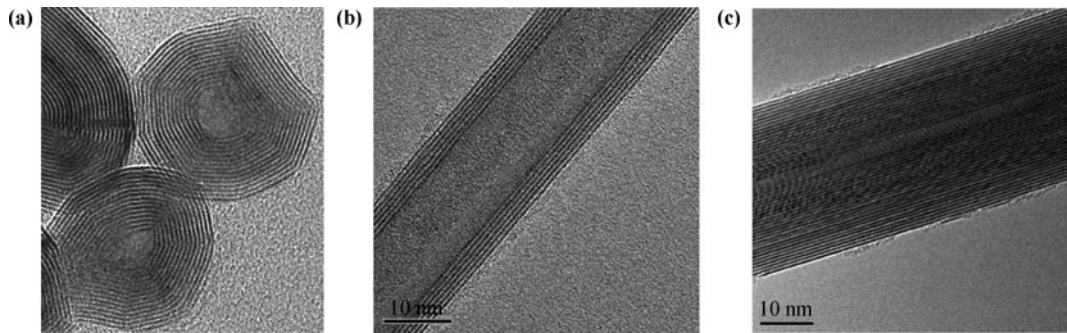


Fig. 1 (a) TEM image of a fullerene-like (IF) nanoparticle of MoS₂; TEM image of a WS₂ nanotube (INT) of type I (b) and II (c). The spacing between the layers is 0.62 nm.

2 Large-scale synthesis of WS₂ nanotubes

The high temperature growth mechanism of the WS₂ nanotubes and MoS₂ from the respective oxides has been investigated since 1995 [3] and 1997 [4] respectively. From early on the purpose of the investigation was, eventually, to develop scalable processes for the synthesis of the nanotubes. Focusing on the synthesis of WS₂ (MoS₂) nanotubes from the respective oxides, it became clear that there are at least two separate mechanisms which could be envisaged. They are depicted schematically in Fig. 2. In the model presented in Fig. 2(a) the nanotubes grow spontaneously in a fast 1D prompting mechanism. Here, MO_{3-x} (M=Mo,W) vapors react with H₂S in a reducing atmosphere yielding a few microns long and narrow (<30 nm) nanotubes within seconds [3, 5] [type I- see Fig. 1(b)]. Significant amounts of WS₂ nanotubes mixed with IF-WS₂ nanoparticles could be obtained in the fluidized bed reactor, developed initially in 2000 for the synthesis of IF-WS₂ nanoparticles [6]. Unfortunately, the

INT-yield of the process was not very high (ca. 5%) and more research is needed to optimize the synthesis.

At the same time, three different groups [7–9] developed independently the two step process [type II- see Fig. 1(c)], whereby in the first step, long W₁₈O₄₇ nanowhiskers grow by heating WO₃ powder in a reducing atmosphere. This reaction is rather fast and is kinetically controlled. In a subsequent reaction, which is mostly diffusion controlled, these nanowhiskers are slowly converted into INT-WS₂ via a reaction with H₂S gas. The next breakthrough came about in 2009 by using a modified fluidized bed reactor in “NanoMaterials, Ltd.” [10, 11]. Meticulous study of the growth parameters provided the path for unifying these two-step synthesis into a combined (one pot) and scalable process, which currently produces about 1/2 kg of multiwall WS₂ nanotubes, daily, in a single batch reaction. Figure 2(b) shows a depiction of the growth mechanism of the type II INT-WS₂. These nanotubes possess quite a perfectly crystalline structure and consequently they exhibit very desirable mechanical properties. Their ultimate strength

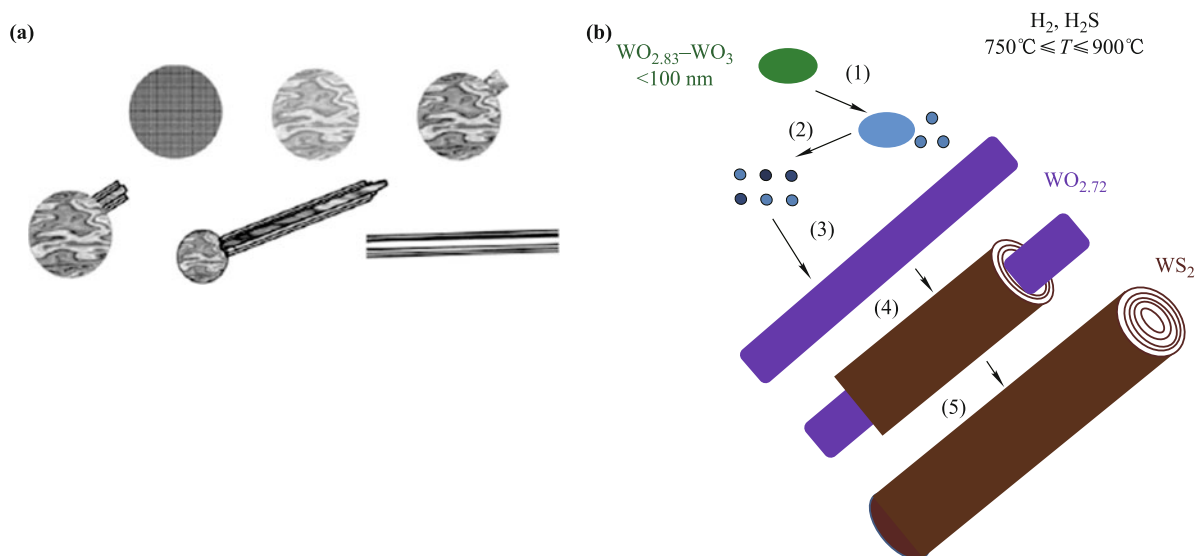


Fig. 2 Schematic rendering of the growth mechanisms of the WS₂ nanotubes: type I (a) and type II (b) nanotubes.

of up to 20 GPa and strain of 10% could be very suitable for reinforcing nanocomposites, as discussed in various recent reports [12, 13].

3 Doping of IF/INT-MoS₂ (WS₂)

The doping of bulk WS₂ and MoS₂ crystals by rhenium atoms was reported in the literature [14, 15]. Rhenium has one extra valence electron as compared to tungsten and molybdenum and could serve as a substitutional donor (n-type conductivity). Contrarily, niobium has one less electron and could serve as p-type dopant. However, for a number of reasons, doping has a different notion in semiconductor nanoparticles as compared to the bulk analogues. Firstly, the conduction band electrons (n-type) or valence band holes do not behave like truly free carriers, as in bulk semiconductors. In fact, due to the mutual repulsion, they are expected to reside in states as close to the surface as possible. Furthermore, the number of extra carriers (or ionized dopant atoms) in the nanocrystal is not sufficient to support a full space-charge layer. Consequently, the potential drop at the surface cannot be fully established and the bands tend to be flattened.

In a series of works, doping of IF-MoS₂ and INT-WS₂ with rhenium atoms has been investigated and its remarkable effect on the rheological and tribological properties of metallic reciprocating surfaces was established [16–19]. The doping of the IF/INT nanoparticles can be done *in-situ* i.e., during the synthesis, or afterwards by annealing the prepared nanoparticles in the presence of the doping agent vapors [16, 17]. The *in-situ* doping process of IF-MoS₂ nanoparticles is an extension of an earlier work, where the synthesis of bulk amounts of the undoped IF-MoS₂ nanoparticles was reported [20]. The major difference between the two syntheses was in the preparation of the molybdenum oxide precursor, which incorporated measured amounts of rhenium oxide. TEM micrograph of a typical Re-doped IF-MoS₂ nanoparticle is shown in Fig. 3. This multiwall hollow closed structure is similar to the undoped IF nanoparticles (compare to Fig. 5 in Ref. [20]). Visibly, the nanoparticle is made out of 30 closed molecular layers of MoS₂ and has a tiny hollow core in the center. Careful chemical analysis was required to evaluate the effective (Re) doping density of the nanoparticles. In fact the optimal doping density of the nanoparticle powder is 100 ppm and below [17]. Combining EXAFS and XANES measurements, the rhenium atom was found to be substitutional to the molybdenum atom, i.e., Re_{Mo} [16] which was confirmed by direct observation of the rhenium atom in the IF-

MoS₂ lattice using high resolution TEM [17]. Recent optical measurements [21] showed systematic blue shift of the A and B exciton peaks in Re-doped IF-MoS₂ as a function of the doping density. The shift was attributed to the Burstein–Moss effect, i.e., band filling due to excess free electrons in the bottom of the conduction band. In fact a good agreement was obtained between the measured/calculated blue shift and the Re-content in the IF-MoS₂ nanoparticles as determined by chemical analysis.

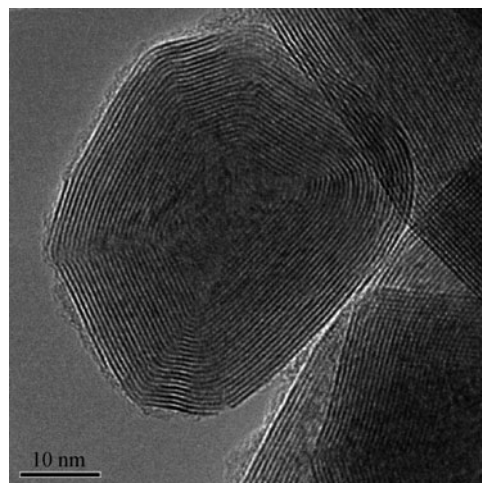


Fig. 3 Typical TEM image of a Re-doped IF-MoS₂ nanoparticle.

The doped nanoparticles exhibit a remarkably different physio-chemical behavior compared with the undoped ones [16–19]. For instance, when taken out of the reactor the powder is very fluffy, due likely to the mutual repulsion between the nanoparticles. When pressed and packed into pellets (for conductivity measurements), unlike their undoped analogues, the product is very fragile and breaks very readily. As expected, the electrical resistivity of the IF-MoS₂ doped powder decreases with the doping density and increases with temperature. Furthermore, the doped nanoparticles form stable suspensions in different solvents. Most importantly, when added to lubricating fluids they lead to the lowest friction and wear among different additives as shown clearly in Fig. 4. This figure depicts two different experimental series done in different places with different settings [18, 19]. The superiority of the Re-doped IF-MoS₂ nanoparticles as solid-state lubricant additive in terms of a reduced friction and wear is clearly demonstrated. More research is needed to understand the detailed *modus operandi* of the doped nanoparticles in tribological interfaces. Nonetheless, these experiments clearly reveal the intimate relationship between electrical and tribological properties of solid lubricants and further extend the potential applications of the IF nanoparticles as superior solid lubricants.

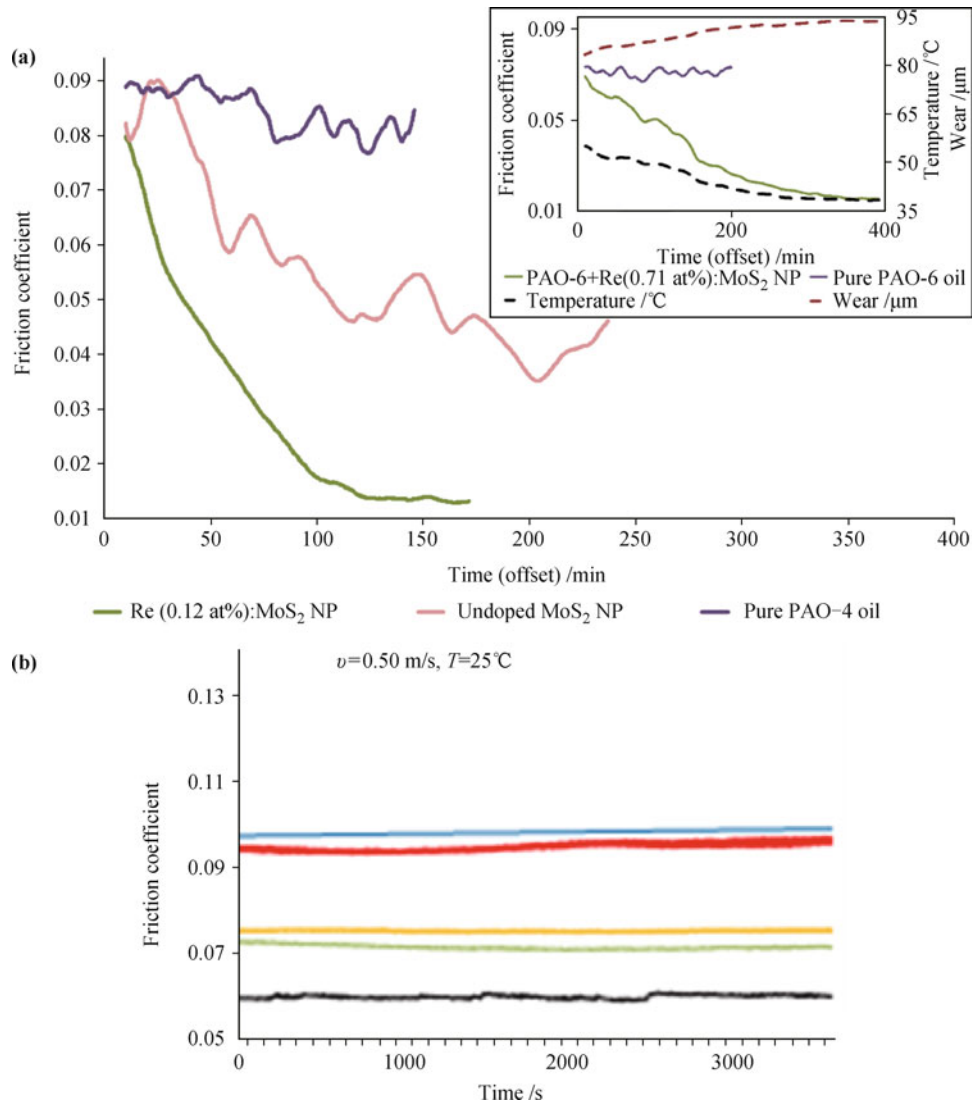


Fig. 4 (a) Friction coefficient vs. time measured with pin-on-disk set-up for different samples in PAO-4 oil with 1 wt% IF nanoparticles. The applied load is 600 N (60 MPa) and the velocity is 0.24 m/s. The inset shows tribological measurements with oil of higher viscosity, i.e., PAO-6. The velocity of the disk here was 0.36 m/s and the load was 615 N (70 MPa). The cumulative wear (*dashed brown curve*) gradually levels off with time. The temperature of the contact area goes gradually down from 53 °C to 28 °C, which is another manifestation for the weak interactions between the reciprocating metals [16]. (b) Evolution of friction coefficient in the ball-on-disc test under mixed lubrication conditions in PAO-6 oil; $p=1.64$ GPa ($L=90$ N); $v=0.5$ m/s. Re:IF-MoS₂ – black; IF-WS₂ – green; IF-MoS₂ – yellow; 2H-MoS₂ – blue; pure PAO-6 – red [19].

4 Catalytic growth of metal-chalcogenide nanotubes

Catalytic growth of nanoparticles, and especially the VLS growth of nanowires has been discussed extensively in the literature [22]. The growth of carbon nanotubes, which is promoted by early transition metal catalysts, like iron and nickel, can be possibly regarded as a hallmark of this chemical strategy. With some notable exemptions though, catalytically promoted growth of inorganic nanotubes did not become a mainstay of this field. Recently, a few examples for heavy metal

catalytic growth of inorganic nanotubes were nevertheless reported [23, 24]. In particular the work of Yella *et al.* [23] serves as an eye-opener, since it focuses on the heavy metals, like bismuth, as catalytic growth promoters. These metals, besides being malleable, are typified by low melting point, in fact much lower than the useful temperature for INT growth. Surprisingly therefore was the observation that temperatures exceeding 2500 K, which were obtained by focused solar beams, could be used to grow MX₂ nanotubes, where M=Mo, W and X=S, Se [24]. Lead was found to be the most suitable catalyst in this case. In fact the high temperatures and temperature gradients in the reaction zone

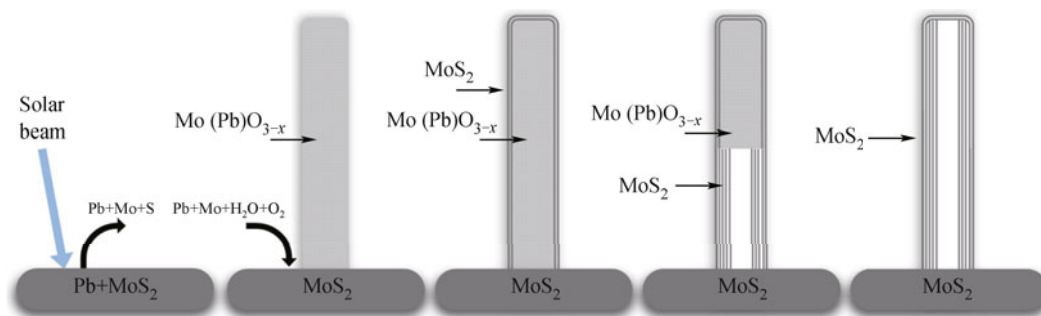


Fig. 5 Schematics of the MoS₂ nanotubes growth in the solar ablation experiment [24].

were critical for the catalytic growth of the MX₂ nanotubes. Although the precise role of the lead catalyst is not fully understood, the current understanding is that it enhances the growth and the thermal stability of the MO_{3-x} nanowhiskers. Figure 5 shows the growth mechanism of the nanotubes [24]. In the first instants of the reaction, the MX₂ powder is converted into MO_{3-x} which protrudes from the sulfide and grows rapidly into a nanowhisker. In the next step, a slow diffusion-controlled back reaction of the oxide nanowhisker with the X₂ vapor leads to the conversion of the nanowhiskers into MX₂ nanotubes. The slow diffusion-controlled back reaction proceeds according to the well-established mechanism described in Refs. [10] and [11].

5 Growth of nanotubes from misfit compounds: (SnS)_n/(SnS₂)_m nanotubes

The first report of IF-SnS₂ nanoparticles obtained by high temperature reaction of SnO₂ nanoparticles and H₂S appeared in Ref. [25]. Later-on, using laser ablation, the production of small amounts of IF and INT of SnS₂ was attempted [26]. However instead of obtaining

the pure SnS₂ nanoparticles, IF and short INT with a sequence of SnS₂ and SnS layers forming a superstructure were obtained. The alternating stacking of the trigonal structure SnS₂ and orthorhombic SnS is reminiscent of misfit compounds of the general formula (MS)_n(TS₂)_m, where M and T are two metal atoms and n, m are real numbers [27, 28]. Misfit compounds have been discussed in the literature since many years. In fact it is well established [29–31] that, due to the lattice mismatch between the orthorhombic (O) MS and the trigonal (T) TS₂ sublattices, at least along one axis, the misfit layers tend to fold and form tubular structures as depicted in Fig. 6 [32]. The stability of the (MS)_n(TS₂)_m superstructure is attributed to a partial charge transfer from the orthorhombic MS to the trigonal TS₂ layer. The large thickness of the (MS)(TS₂) layer (above 1 nm in the simplest case of $n = m = 1$) does not allow these tubes to adopt diameters smaller than one micron, in general. However, by combining the effect of misfit; heavy metal catalysts and the edge annihilation effect as manifested by other INT, one could hope to form misfit nanotubes with diameters as small as 100 nm and even below [27, 28]. Figure 7 shows a TEM picture of a (SnS)(SnS₂) nanotube obtained by annealing SnS₂ powder in the presence

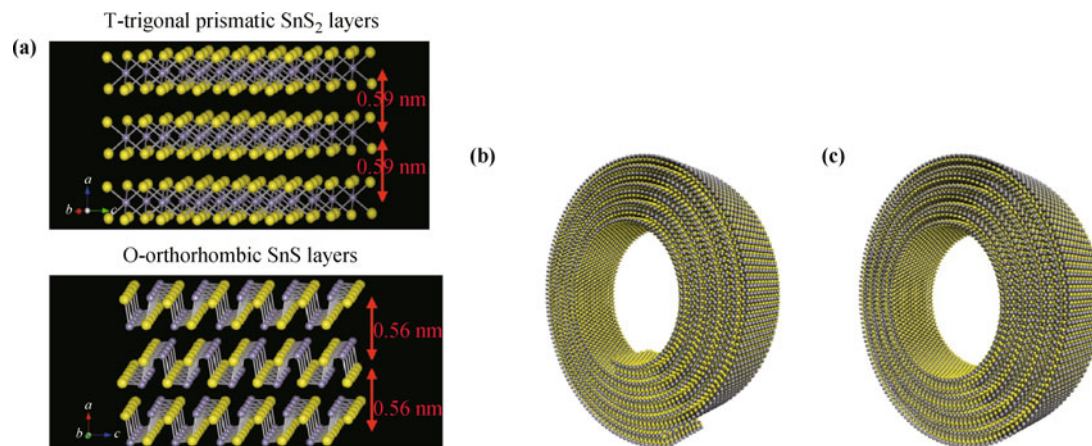


Fig. 6 (a) Schematic rendering of the lattice structure of the trigonal (T) SnS₂ and orthorhombic (O) SnS; (b) Scrolling of the misfit O-T layers of SnS-SnS₂; (c) Remediation of the edges during the annealing process leads to the formation of crystalline O-T misfit nanotubes (courtesy of Dr. A. N. Enyashin, RAS, Ekaterinburg).

of Bi and Sb_2S_3 as growth promoters. A large temperature gradient was applied in this case with the precursors placed at 800°C and the product was collected at 250°C . Misfit nanotubes with the superstructure order O-T ($\text{SnS}(\text{SnS}_2)$), O-T-T ($\text{SnS}(\text{SnS}_2)_2$), and O-O-T-T-T ($\text{SnS}_2(\text{SnS}_2)_3$), were also analyzed in the reaction products [27, 28].

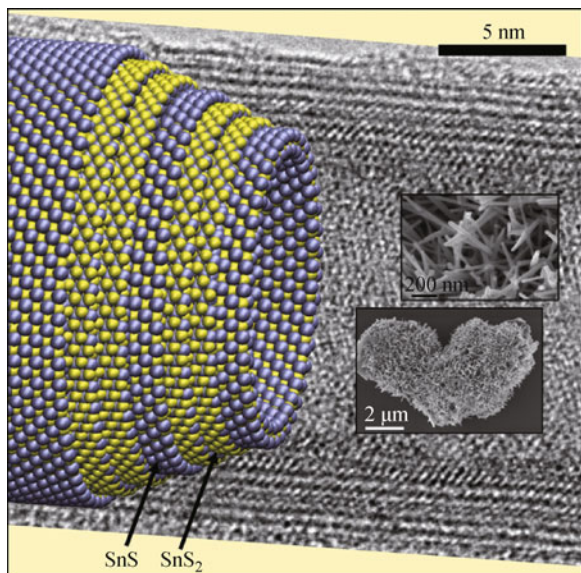


Fig. 7 TEM image of O-T-T ($\text{SnS-SnS}_2\text{-SnS}_2$) misfit nanotube. Superimposed on the TEM image is a model showing the lattice structure of this misfit nanotube (courtesy of Dr. A. N. Enyashin, RAS, Ekaterinburg). The insets show SEM images of an assortment of misfit nanotubes in two magnifications.

The growth mechanism of these nanotubes involved, most likely, first formation of the misfit nanosheet. This step was strongly promoted by the bismuth and antimony catalysts. It was hypothesized that the role of the bismuth, at least in part, is to dislodge some sulfur atoms from the SnS_2 precursor by forming Bi_2S_3 obtaining thereby the orthorhombic SnS layers. Subsequently, the misfit sheet formed a nanoscroll which after some further annealing was converted into a perfect nanotube by annealing-out the edges. One can thus regard these misfit nanotubes as a new “templating” strategy, where the lattice-mismatch between the two molecular sheets; the partial charge transfer between the layers and the catalytic reaction serves as the stimulus for folding of the layers. Subsequently, the nanoscrolls are converted into nanotubes by annealing-out the rim atoms.

6 Core-shell nanotubes

Filling of the hollow core of carbon nanotubes has been the subject of numerous studies. There are variety of

reasons why one would like to use this hollow space, for instance for drug delivery purposes; reinforcing the nanotube, or for the understanding of materials’ crystallization under confined space [33]. It was hypothesized, that the wider hollow core of inorganic nanotubes could serve the purpose of forming a template for the crystallization of nanotubes from other layered compounds, which cannot be easily formed otherwise. For that purpose a drop of, e.g. PbI_2 salt was melted near the WS_2 nanotubes at 500°C . The strong capillary forces and the covalent nature of the chemical bond in this salt lead to a perfect wetting of the inner core of the WS_2 nanotube. Upon cooling, the receding salt crystallized forming a perfect core-shell $\text{PbI}_2@WS_2$ nanotubular structure as shown in Fig. 8 [34, 35]. This strategy was later exploited for the synthesis of other core-shell-based iodide salts, like BiI_3 and AsI_3 inside the hollow core of WS_2 nanotubes. Theoretical calculations indicated that, due to the elastic strain, the innermost layer of the core nanotube cannot go below say 5 nm, which was confirmed by the experiments. In order to extend this templating strategy to

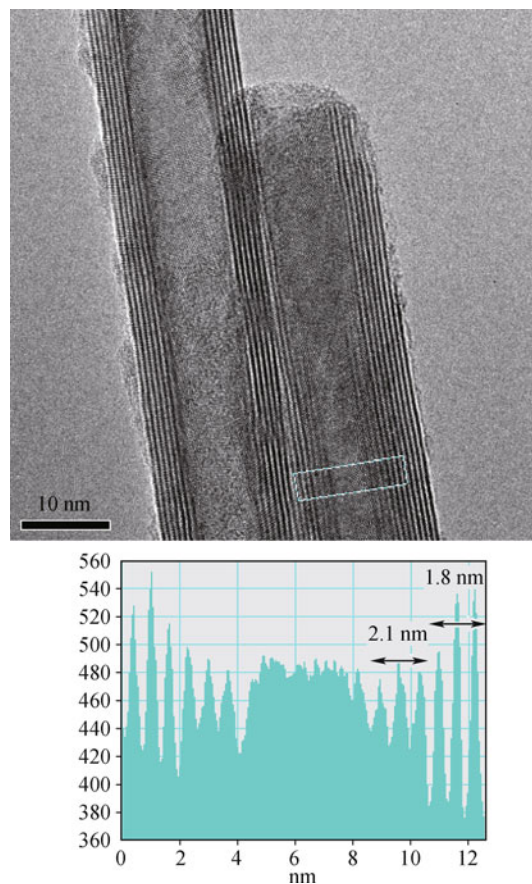


Fig. 8 TEM micrograph of core-shell $\text{PbI}_2@WS_2$ nanotubes. The inner PbI_2 nanotube has a periodicity of 0.7 nm and the templating (outer) WS_2 nanotube a periodicity of 0.6 nm as shown by the line profile.

salts with larger ionic character, like the metal-chlorides, one needs to use template (nanotubes) with higher degree of ionicity which cannot be easily synthesized so far.

7 Applications

Various applications have been proposed for inorganic nanotubes and fullerene-like nanostructures. Extensive research and development effort was carried out to capitalize on their superior behavior as solid lubricants [36]. While a fair number of products are already on the market place (see for example Ref. [37]), mostly as additive to lubricating oils, additional work is needed to extend this concept to many other products and technologies. The main obstacle is the tendency of the nanoparticles to agglomerate, on the one hand and their compatibility with the existing technology, like formulated oils, greases etc., on the other hand. Self-lubricating coatings containing the nanoparticles have been prepared and were shown to be suitable for variety of applications [38], including orthodontic wires; endodontic files and medical insertion devices. The addition of small amounts of IF/INT into high performance polymer matrices was shown to bring about a significant reinforcement effect; improved tribological behavior and increased thermal stability of the nanocomposites [12, 13]. Apparently, on top of being good solid lubricants and mechanically very robust, the IF nanoparticles lead to improved rheological properties of the polymer blends [39, 40]. Therefore, mixing the IF with other additives, like carbon fibers and nanotubes into the polymer matrix produces a strong synergistic effect [39, 40] and could lead to improved nanocomposites-based technologies.

Various other applications are currently under investigation which could offer a large number of new technologies in the future.

Acknowledgements I am grateful to all my collaborators and students who contributed to this publication, including Prof. M. Levy, Drs. R. Popovitz-Biro, R. Rosentsveig, R. Kreizman, A. Albu-Yaron, Ms. L. Yadgarov, Ms. O. Brontvein, Mr. G. Radovsky. R. Tenne acknowledges the support of the ERC (project INTIF 226639), the Israel Science Foundation; the Harold Perlman Foundation; the Irving and Azelle Waltcher Research Fund and the Irving and Cherna Moskowitz Center for Nano and Bio-Nano Imaging. He is the director of the Helen and Martin Kimmel Center for Nanoscale Science and holds the Drake Family Chair in Nanotechnology.

References and notes

1. R. Tenne, L. Margulis, M. Genut, and G. Hodes, Polyhedral and cylindrical structures of tungsten disulphide, *Nature*, 1992, 360(6403): 444
2. L. Margulis, G. Salitra, R. Tenne, and M. Talianker, Nested fullerene-like structures, *Nature*, 1993, 365(6442): 113
3. Y. Feldman, E. Wasserman, D. J. Srolovitz, and R. Tenne, High-rate, gas-phase growth of MoS₂ nested inorganic fullerenes and nanotubes, *Science*, 1995, 267(5195): 222
4. M. Homyonfer, B. Alpers, Yu. Rosenberg, L. Sapir, S. R. Cohen, G. Hodes, and R. Tenne, Intercalation of inorganic fullerene-like structures yields photosensitive films and new tips for scanning probe microscopy, *J. Am. Chem. Soc.*, 1997, 119(11): 2693
5. R. Rosentsveig, A. Margolin, Y. Feldman, R. Popovitz-Biro, and R. Tenne, WS₂ nanotube bundles and foils, *Chem. Mater.*, 2002, 14(2): 471
6. Y. Feldman, A. Zak, R. Popovitz-Biro, and R. Tenne, New reactor for production of tungsten disulfide hollow onion-like (inorganic fullerene-like) nanoparticles, *Solid State Sci.*, 2000, 2(6): 663
7. Y. Q. Zhu, W. K. Hsu, N. Grobert, B. H. Chang, M. Terrones, H. Terrones, H. W. Kroto, D. R. M. Walton, and B. Q. Wei, Production of WS₂ nanotubes, *Chem. Mater.*, 2000, 12(5): 1190
8. H. A. Therese, J. Li, U. Kolb, and W. Tremel, Facile large scale synthesis of WS₂ nanotubes from WO₃ nanorods prepared by a hydrothermal route, *Solid State Sci.*, 2005, 7(1): 67
9. A. Rothschild, J. Sloan, and R. Tenne, Growth of WS₂ nanotubes phases, *J. Am. Chem. Soc.*, 2000, 122(21): 5169
10. A. Zak, L. Sallacan-Ecker, A. Margolin, M. Genut, and R. Tenne, Insight into the growth mechanism of WS₂ nanotubes in the scaled-up fluidized-bed reactor, *Nano*, 2009, 4(02): 91
11. A. Zak, L. Sallacan Ecker, R. Efrati, L. Drangai, N. Fleischer, and R. Tenne, Large-scale synthesis of WS₂ multi-wall nanotubes and their dispersion, an update, *Sensors & Transducers J.*, 2011, 12: 1
12. E. Zohar, S. Baruch, M. Shneider, H. Dodiuk, S. Kenig, H. D. Wagner, A. Zak, A. Moshkovith, L. Rapoport, and R. Tenne, The mechanical and tribological properties of epoxy nanocomposites with WS₂ nanotubes, *Sensors & Transducers J.*, 2011, 12: 53
13. M. Naffakh, M. Remskar, C. Marco, and M. A. Gómez-Fatou, Dynamic crystallization kinetics and nucleation parameters of a new generation of nanocomposites based on isotactic polypropylene and MoS₂ inorganic nanotubes, *J. Phys. Chem. B*, 2011, 115(12): 2850
14. K. Tiong, P. Liao, C. Ho, and Y. Huang, Growth and characterization of rhenium-doped MoS₂ single crystals, *J. Cryst. Growth*, 1999, 205(4): 543
15. P. Yen, Y. Huang, and K. Tiong, The growth and characterization of rhenium-doped WS₂ single crystals, *J. Phys.: Condens. Matter*, 2004, 16(12): 2171
16. L. Yadgarov, R. Rosentsveig, G. Leituss, A. Albu-Yaron, A. Moshkovith, V. Perflyev, R. Vasic, A. I. Frenkel, A. N.

- Enyashin, G. Seifert, L. Rapoport, and R. Tenne, Controlled doping of MS_2 ($M=W, Mo$) nanotubes and fullerene-like nanoparticles, *Angew. Chem. Int. Ed.*, 2012, 51(5): 1148
17. L. Yadgarov, D. G. Stroppa, R. Rosentsveig, R. Ron, A. N. Enyashin, L. Houben, and R. Tenne, Investigation of rhenium-doped MoS_2 nanoparticles with fullerene-like structure, *Z. Anorg. Allg. Chem.*, 2012, 638(15): 2610
 18. L. Rapoport, A. Moshkovich, V. Perfiliev, A. Laikhtman, I. Lapsker, L. Yadgarov, R. Rosentsveig, and R. Tenne, High lubricity of Re-doped fullerene-like MoS_2 nanoparticles, *Tribol. Lett.*, 2012, 45(2): 257
 19. L. Yadgarov, V. Petrone, R. Rosentsveig, Y. Feldman, R. Tenne, and A. Senatore, Tribological studies of rhenium doped fullerene-like MoS_2 nanoparticles in boundary, mixed and elasto-hydrodynamic lubrication conditions, *Wear*, 2013, 297(1–2): 1103
 20. R. Rosentsveig, A. Margolin, A. Gorodnev, R. Popovitz-Biro, Y. Feldman, L. Rapoport, G. R. Samorodnitsky-Naveh, and R. Tenne, Synthesis of fullerene-like MoS_2 nanoparticles and their tribological behavior, *J. Mater. Chem.*, 2009, 19(25): 4368
 21. Q. C. Sun, L. Yadgarov, R. Rosentsveig, G. Seifert, R. Tenne, and J. L. Musfeldt, Observation of a Burstein–Moss shift in rhenium-doped MoS_2 nanoparticles, *ACS Nano*, 2013, 7(4): 3506
 22. A. M. Morales and C. M. Lieber, A laser ablation method for the synthesis of crystalline semiconductor nanowires, *Science*, 1998, 279(5348): 208
 23. A. Yella, E. Mugnaioli, M. Panthofer, H. A. Therese, U. Kolb, and W. Tremel, Bismuth-catalyzed growth of SnS_2 nanotubes and their stability, *Angew. Chem. Int. Ed.*, 2009, 48(35): 6426
 24. O. Brontvein, D. G. Stroppa, R. Popovitz-Biro, A. Albu-Yaron, M. Levy, D. Feuerman, L. Houben, R. Tenne, and J. M. Gordon, New high-temperature Pb-catalyzed synthesis of inorganic nanotubes, *J. Am. Chem. Soc.*, 2012, 134(39): 16379
 25. B. Alpers, M. Homyonfer, and R. Tenne, Photoelectrochemical studies with inorganic cage structures of metal dichalcogenides, *J. Electroanal. Chem.*, 1999, 473(1–2): 186
 26. S. Y. Hong, R. Popovitz-Biro, Y. Prior, and R. Tenne, Synthesis of SnS_2/SnS fullerene-like nanoparticles: A superlattice with polyhedral shape, *J. Am. Chem. Soc.*, 2003, 125(34): 10470
 27. G. Radovsky, R. Popovitz-Biro, M. Staiger, K. Gartsman, C. Thomsen, T. Lorenz, G. Seifert, and R. Tenne, Synthesis of copious amounts of SnS_2 and SnS_2/SnS nanotubes with ordered superstructures, *Angew. Chem. Int. Ed.*, 2011, 50(51): 12316
 28. G. Radovsky, R. Popovitz-Biro, and R. Tenne, Study of tubular structures of the misfit layered compound SnS_2/SnS , *Chem. Mater.*, 2012, 24(15): 3004
 29. A. Meerschaut, Misfit layer compounds, *Curr. Opin. Solid State & Mater. Sci.*, 1996, 1(2): 250
 30. J. Rouxel and A. Meerecheut, Misfit layer compounds $(MX)_n(TX_2)_m$ [$M=Sn, Pb, Bi$, Rare earth; $T=$ Transition metal; $X=S, Se$; $1.08 < n < 1.25$; $m=1, 2$], *Mol. Cryst. Liq. Cryst. Sci. Tec. A*, 1994, 244(1): 343
 31. G. A. Wiegers and A. Meerschaut, Misfit layer compounds $(MS)_nTS_2$ ($M=Sn, Pb, Bi$, Rare earth metals; $T=Nb, Ta, Ti, V, Cr$; $1.08 < n < 1.23$): Structures and physical properties, *Mater. Sci. Forum*, 1992, 100–101: 101
 32. D. Bernaerts, S. Amelinckx, G. Van Tendeloo, and J. Van Landuyt, Microstructure and formation mechanism of cylindrical and conical scrolls of the misfit layer compounds $PbNb_nSn_{2n+1}$, *J. Cryst. Growth*, 1997, 172(3–4): 433
 33. E. Philp, J. Sloan, A. I. Kirkland, R. R. Meyer, S. Friedrichs, J. L. Hutchison, and M. L. H. Green, An encapsulated helical one-dimensional cobalt iodide nanostructure, *Nat. Mater.*, 2003, 2(12): 788
 34. R. Kreizman, S. Y. Hong, J. Sloan, R. Popovitz-Biro, A. Albu-Yaron, G. Tobias, B. Ballesteros, B. G. Davis, M. L. H. Green, and R. Tenne, Core-shell $PbI_2@WS_2$ inorganic nanotubes from capillary wetting, *Angew. Chem. Int. Ed.*, 2009, 48(7): 1230
 35. R. Kreizman, A. N. Enyashin, F. L. Deepak, A. Albu-Yaron, R. Popovitz-Biro, G. Seifert, and R. Tenne, Synthesis of core-shell inorganic nanotubes, *Adv. Funct. Mater.*, 2010, 20(15): 2459
 36. L. Rapoport, Yu. Bilik, Y. Feldman, M. Homyonfer, S. R. Cohen, and R. Tenne, Hollow nanoparticles of WS_2 as potential solid-state lubricants, *Nature*, 1997, 387: 791
 37. VA237 and VA267 bearings in SKF catalog: <http://www.skf.com/group/products/bearings-units-housings/engineered-products/skf-drylube-bearings/designation-system/index.html>
 38. A. R. Adini, M. Redlich, and R. Tenne, Medical applications of inorganic fullerene-like nanoparticles, *J. Mater. Chem.*, 2011, 21(39): 15121
 39. A. M. Díez-Pascual, M. Naffakh, C. Marco, and G. Ellis, Rheological and tribological properties of carbon nanotube/thermoplastic nanocomposites incorporating inorganic fullerene-like WS_2 nanoparticles, *J. Phys. Chem. B*, 2012, 116(27): 7959
 40. A. M. Díez-Pascual, M. Naffakh, C. Marco, and G. Ellis, Mechanical and electrical properties of carbon nanotube/poly(phenylene sulphide) composites incorporating polyetherimide and inorganic fullerene-like nanoparticles, *Composites: Part A*, 2012, 43: 603